Electron temperature diagnostics of aluminium plasma in a z-pinch experiment at the "QiangGuang-1" facility*

Li Mo(李 沫)†, Wu Jian(吴 坚), Wang Liang-Ping(王亮平), Wu Gang(吴 刚), Han Juan-Juan(韩娟娟), Guo Ning(郭 宁), and Qiu Meng-Tong(邱孟通)

Northwest Institute of Nuclear Technology, Xi'an 710024, *China*

(Received 2 May 2012; revised manuscript received 30 May 2012)

Two curved crystal spectrometers are set up on the "QiangGuang-1" generator to measure the z-pinch plasma spectra emitted from planar aluminum wire array loads. Kodak Biomax-MS film and an IRD AXUVHS5# array are employed to record time-integrated and time-resolved free-bound radiation, respectively. The photon energy recorded by each detector is ascertained by using the L-shell lines of molybdenum plasma. Based on the exponential relation between the continuum power and photon energies, the aluminum plasma electron temperatures are measured. For the time-integrated diagnosis, several "bright spots" indicate electron temperatures between (450 eV$\sim$ 520 eV) $\pm$ 35%. And for the time-resolved ones, the result shows that the electron temperature reaches about 800 eV $\pm$ 30% at peak power. The system satisfies the demand of z-pinch plasma electron temperature diagnosis on a $\sim$ 1 MA facility.

Keywords: electron temperature, continuum, curved crystal spectrometer, z-pinch

PACS: 52.70.La, 32.30.Rj **DOI:** 10.1088/1674-1056/21/12/125202

1. Introduction

Electron temperature, as well as electron density, are key parameters for understanding plasma sources and plasma processing. Accurate and reliable measurement of the electron temperature is an important step in most plasma related research. Knowledge of the time-dependent electron temperature in z-pinch is required in order to understand pinch dynamics and radiation generation.[1−4]

Diagnostics through the radiation spectrum is a main way to measure a plasma's electron temperature. For a Maxwellian plasma of electron temperature T_e, the energy spectrum of the free-bound (FB) X rays is proportional to exp $(-E/T_e)$, where E is X-ray photon energy.[5−7] A time-dependent electron temperature diagnostic based on this principle was applied to $\sim$ 30 TW aluminum z-pinch plasma generated by imploding large-wire-number arrays on the Saturn accelerator (6.9 MA, 35 ns).[8] Seven filtered diamond photoconducting detectors (PCD) were used to measure the FB continuum and hence the time-resolved electron temperature on the axis was fitted. The measurement of the free-bound X-rays from the highly-stripped, K-shell aluminum ions provides a model-independent measurement of the core electron temperature, owing to the long X-ray mean-free-path. However, the same system can hardly be used on $\sim$ 1-MA facilities due to the low X-ray radiation power and abrupt continuum slope.

In this paper, we show the measurement of electron temperature at the "QiangGuang-1" facility ($\sim$ 1.3 MA, 80 ns$\sim$100 ns). Two spectrometers are employed to measure the spectra emitted from an aluminum wire array z-pinch. Time-integrated and time-resolved electron temperatures are measured from the FB continuum slope. The method provides a new option to diagnose electron temperatures of high power wire array z-pinches on $\sim$ 1-MA facilities.

2. Experimental setup

"QiangGuang-1" is a pulsed power machine with linear-transformer-driver (LTD) based water-dielectric low impedance transmission lines. The LTD consists of 120 4-μF/50 kV capacitors, and has a maximum energy storage of 600 kJ. The water-dielectric lines are composed of a 1.4-Ω intermediate line, a transmission line, and an output line.[9] In experiment, "QiangGuang-1" provides a peak current of $\sim$ 1.3 MA with a 10%–90% rise time of $\sim$ 80 ns.

*Project supported by the Young Scientists Fund of the National Natural Science Foundation of China (Grant No. 10905047).

†Corresponding author. E-mail: lemon7665@sina.com

© 2012 Chinese Physical Society and IOP Publishing Ltd

The loads used in the experiment were all double-planar wire arrays (DPWAs). Each load consisted of two rows of 15-μm aluminum wires, each wire was 20 mm in length, and each row contained ten wires. The interwire gap was 0.9 mm, and the interrow gap was 4.5 mm. The total mass of each DPWA was 191 μg/cm. In experiment the X-ray pulse was generated from these arrays with a high reproducibility.

Two side-on spectrometers were employed to measure FB radiation. One elliptical-curved thallium acid phthalate (TlAP $2d = 2.576$ nm) crystal spectrometer provided time-integrated (and spatially resolved) spectrum with a film pack. It covers the energy range from 1.9 keV to 3 keV. The other was a convex-curved TlAP crystal spectrometer measuring time-resolved (and spatially integrated) spectrum with a diode-array. A compound filter composed of 36-μm polypropylene (PP), 2.5-μm terephthalate (Mylar), and 0.4-μm aluminum was set on each spectrometer to protect the crystal from hitting by the debris. The compound filter is a substitute for ∼ 80-μm beryllium, which is toxic and hard to handle.

Photoconducting detectors (PCDs) were used to monitor the time-resolved extreme ultraviolet (XUV) and soft X-ray power in a number of wavelength bands of interest. A side-on eight-frame pinhole camera was employed to monitor the time-gated X-ray emission with a frame duration of ∼ 5 ns. The spatial resolution of the camera is ∼ 400 μm because of the large pinhole diameter (100 μm) and the low magnification factor (0.31). Al K-shell spectra were measured by using a four-frame time-gated curved TlAP spectrometer with a spectral resolution ($\lambda/\Delta\lambda$) of ∼ 500.[10]

3. Experimental results

3.1. Time-integrated diagnosis

Figure 1 shows three typical time-integrated spectra from a planar Al wire array z-pinch and the Mo L-shell spectrum from an Mo wire array x-pinch. All the spectra were produced by the elliptical-curved TlAP crystal spectrometer with Kodak Biomax-MS films. In the upper three images, the vertical direction is parallel to the pinch axis and spatially resolved using a 20-μm wide slit. Photons with different energies are dispersed along the horizontal direction. The direction from the cathode (labeled "C") to anode (labeled "A") is marked. The Mo x-pinch spectrum was taken by the spectrometer with a 2-mm wide slit.

All the spectra are of first-order Bragg reflections. Since the actual surface formula of the crystal is inevitably different from the design, it is necessary to ascertain wavelength corresponding to the pixels on the film. The spectrometer was designed to cover the parts of H-like and He-like lines of Al. The Mo L-shell lines are in the spectral region taken by the spectrometer and are coterminous in wavelength with Al. So one shot with a Mo x-pinch load was tested on the facility (see Fig. 1). Photon energies for selected transitions of Al H-like, He-like, and Mo Ne-like presented in Fig. 1 are shown in Table 1. Energies are taken from the National Institute of Standards and Technology (NIST).

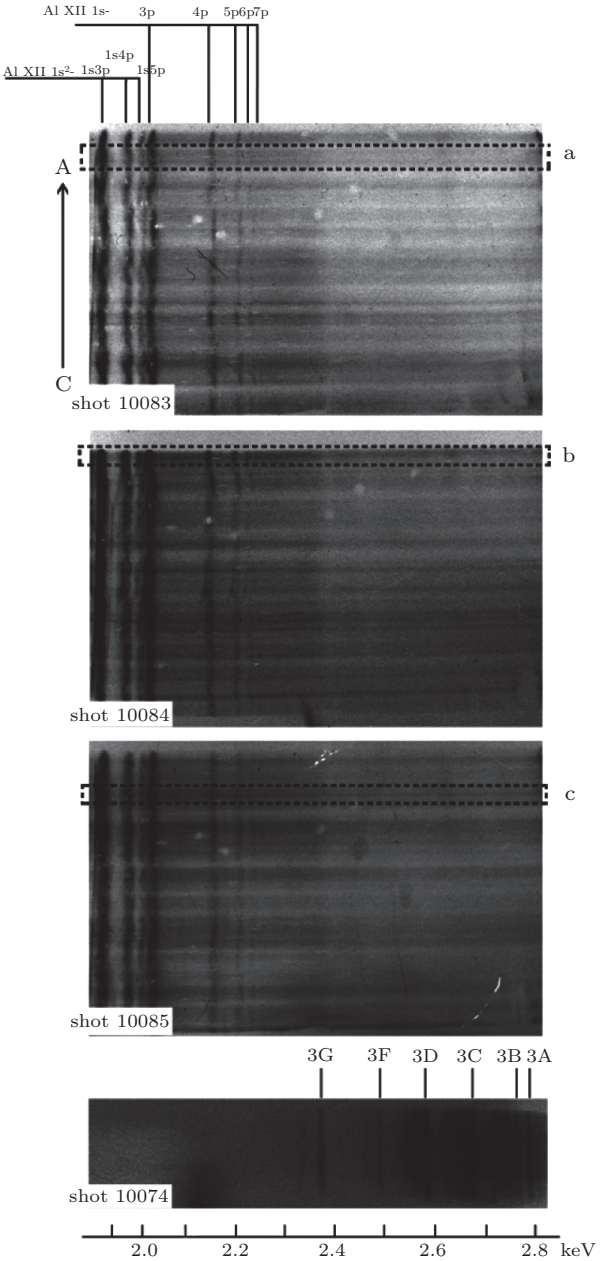


Fig. 1. Typical spectra from 20-wire, 15-μm planar Al wire arrays z-pinches and Mo wire arrays x-pinch.

There are two intense sources of radiation during stagnation: Al XII line emission from a precursor-sized object, and both continuum and Al XIII radiation from bright spots of either significantly higher temperature or density randomly distributed around this object, thereby producing a hollow emission profile.[11]

Since the continuum emission originates mainly from bright spots, then only discontinuous electron temperature along the pinch axis can be measured from the time-integrated spectra. One bright spot radiation from each Al z-pinch shot was analysed as shown in Fig. 1. The transmission ratio of the complex filter was calculated using the mass absorption coefficient given in Ref. [5]. The integral diffraction efficiency of TlAP crystal in the X-ray energy range 2100 eV–5600 eV was measured on beamline 4B7 at the Beijing Synchrotron Radiation Facility.[12,13] The result shows that it is quite close to the calculation result from the "Darwin Prins" model (which is for perfect crystals).[14] The response of Kodak Biomax-MS film was calculated using the double-emulsion model.[15,16] Figure 2 shows the integrated reflection efficiency of the crystal, filter transmission ratio, and their product. Figure 3 shows the normalized spectrum from the marked bright spot of shot 10084. The obvious false peak in the spectrum curve near 2400 eV was caused by the absorption edge of thallium with no calibration data.[12,13] Thus electron temperature was calculated using data between 2500 eV∼2850 eV. All electron temperatures from three bright spots are listed in Table 2. The uncertainty is about 35%.

Table 1. Energies for Al and Mo lines presented in Fig. 1.

Ion		Configurations	Terms	NIST energy
Mo XXXIII	3A	$2s^22p^6$-$2s2p^63p$	1P1	2806.1 eV
	3B		3P1	2776.7 eV
	3C	$2s^22p^6$-$2s^22p^53d$	1P1	2676.4 eV
	3D		3D1	2580.6 eV
	3F	$2s^22p^6$-$2s^22p^53s$	1P1	2488.2 eV
	3G		3P1	2381.1 eV
Al III		1s-6p	2P	2240.2 eV
		1s-5p	2P	2212.1 eV
		1s-4p	2P	2160.3 eV
		1s-3p	2P	2048.5 eV
Al II		$1s^2$-1s5p	1P	2007.7 eV
		$1s^2$-1s4p	1P	1963.7 eV
		$1s^2$-1s3p	1P	1868.7 eV

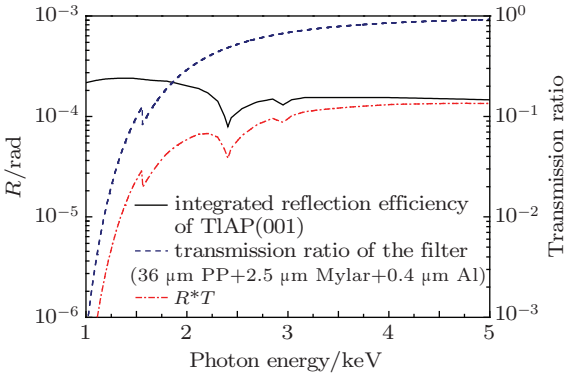


Fig. 2. (color online) Integrated reflection efficiency of TlAP(001) crystal, transmission ratio of the compound filter, and their product.

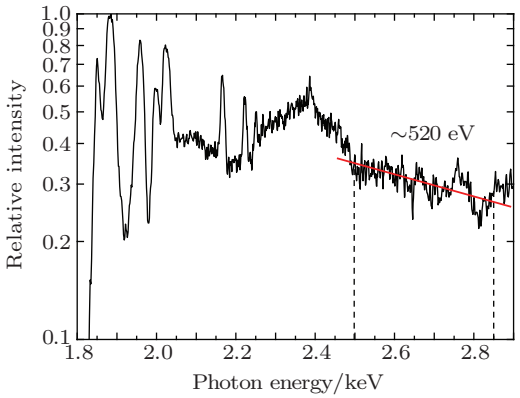


Fig. 3. (color online) Normalized spectrum from the bright spot of shot 10084 shown in Fig. 1.

Table 2. Calculated bright spot electron temperatures of the area shown in Fig. 1.

Area	Shot No.	I_{max}/MA	T_e/eV
a	10083	1.23	∼ 510
b	10084	1.29	∼ 520
c	10085	1.21	∼ 450

3.2. Time-resloved diagnosis

The convex-curved crystal spectrometer was equipped with an R=100 mm TlAP crystal. An International Radiation Detectors (IRD) AXUVHS5# (with 100-μm sensitive layer thickness. Its responsivity is shown in Fig. 4.) array was employed to record the time-resolved radiation signals. The detectors are sensitive to radiation from 7 eV to 6000 eV. Each diode has a response time of 1 ns and a sensitivity of about 0.27 A/W.[17,18] Calibration of one diode sensitivity was done by IRD Inc. The difference between theory and calibration data is less than 1%.

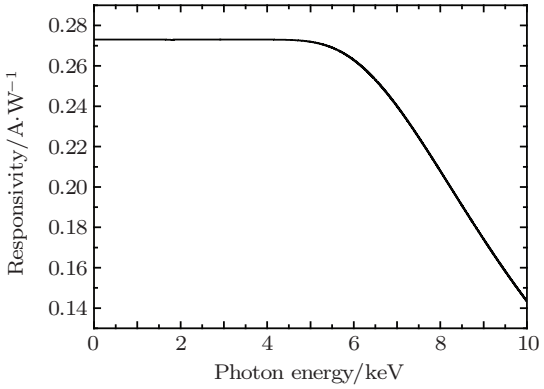


Fig. 4. Responsivity of the AXUVHS5# detector with 100-μm sensitive layer thickness.

It is unfortunate that by the time the experiment began only two of the detectors were useable because of their brittle structure. Thus only two photon energy points on the continuum could be measured. To confirm the two photon energies recorded by each photodiode, an Mo x-pinch load was tested on the accelerator. The time-integrated Mo L-shell spectrum was taken with a Kodak Biomax-MS film which was arranged on the plane of the two detectors. The positions of the detectors were marked on the film [see Fig. 5]. The central photon energies received by the diodes are 2695 eV and 3395 eV, respectively.

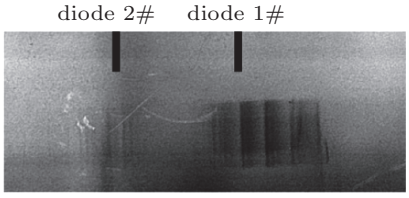


Fig. 5. Time-integrated X-ray spectroscopy from shot 11169 (24-wire 30-μm Mo x-pinch).

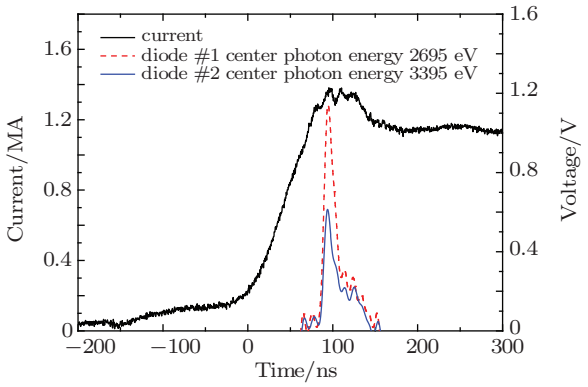


Fig. 6. (color online) Current data and signals of the photodiodes from shot 11121 (20-wire 15-μm Al planar load).

For shot 11121, a DPWA load was tested on the "QiangGuang-1" facility. The current waveform and two diode waveforms are shown in Fig. 6. Signals were filtered by a 100-MHz low pass filter to reduce electromagnetic disturbance.

The time-resolved electron temperature near the peak power of shot 11121 was calculated [see Fig. 7]. The result indicates that the electron temperature is about 800 eV when the plasma stagnated. For the rest of the time it is hard to compute because of the electromagnetic disturbance.

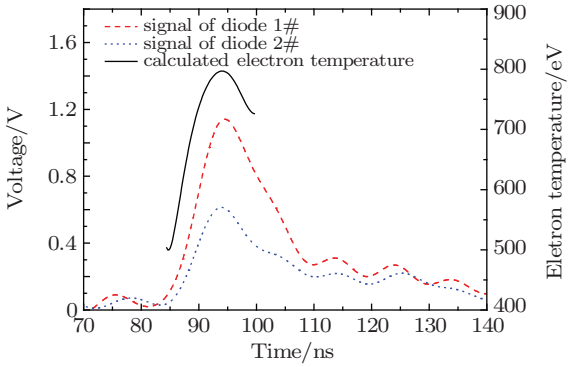


Fig. 7. (color online) Detector signals and the calculated electron temperatures for shot 11121.

The uncertainty of the electron temperature diagnostics comes mainly from two sources: the difference between the real integrated reflection efficiency and the calculated integrated reflection efficiency of TlAP crystal and also the discrepancy in relative response between the two photodiodes. The total uncertainty is about 30%.

4. Conclusion and discussion

Electron temperatures of aluminum plasma generated by the "QiangGuang-1" facility are measured with curved crystal spectrometers which cover the continuum spectrum range. Time-integrated spectra show that continuum emission originates from bright spots with electron temperatures of about 500 eV. Time-resloved electron temperatures are given by measuring powers of two photon energies of the continuum emission. The data gives an electron temperature of 800 eV at peak power.

Electron temperature can also be estimated by line ratios. Time-integrated and time-gated Al K-shell lines are recorded by the four-frame time-gated curved TlAP spectrometer. The He-β/(He-α+IC) line ratio is a function of electron temperature and ion density. The time-integrated electron temperature along the z axis is between 400 eV and 700 eV analysed from tables in Ref. [19]. Also time-gated spectra show that

the electron temperature can reach 800 eV or more. Ion density is estimated as follows: for a 191-μg/cm load all compressed in a 1-mm radii plasma cylinder, the ion density is 1.35×10^{20} cm^{-3}. So the density could be 6×10^{19} cm$^{-3}\sim7\times10^{19}$ cm^{-3} in the stagnation period, and 50%∼60% of the total material is involved in the implosion.[11] Time-integrated ion density is estimated to be 2×10^{19} cm^{-3}.

There is no accurate diagnosis for measuring ion density on the "QiangGuang-1" facility. Nevertheless, the method based on continuum emission can provide a more accurate measurement than the method using line ratios.

References

[1] Xiao D L, Ning C, Lan K and Ding N 2010 *Acta Phys. Sin.* **59** 430 (in Chinese)

[2] Li J, Xie W P, Huang X B, Yang L B, Cai H C and Pu Y K 2010 *Acta Phys. Sin.* **59** 7922 (in Chinese)

[3] Sanford T W L, Nash T J, Mock R C, Spielman R B, Struve K W, Hammer J H, DeGroot J S, Whitney K G and Apruzese J P 1997 *Phys. Plasmas* **4** 2188

[4] Ryutov D D, Derzon M S and Matzen M K 2000 *Rev. Mod. Phys.* **72** 167

[5] Hutchinson I H 2002 *Principles of Plasma Diagnostics* (Cambridge: Cambridge University Press) p. 201

[6] Fujimoto T 2004 *Plasma Spectroscopy* (Oxford: Clarendon Press) p. 205

[7] Gross B, Grycz B and Miklóssy K 1980 *Plasma Technology* (Beijing: Science Press) p. 136 (in Chinese)

[8] Sanford T W L, Nash T J, Mock R C, Spielman R B, Seamen J F, McGurn J S, Whitney K G, Thornhill J W, Pulsifer P E and Apruzese J P 1997 *Rev. Sci. Instrum.* **68** 852

[9] Zeng Z Z, Qiu M T, Cong P T, Wang L P, Kuai B, Sheng L, Wu G, Guo N, Li H and Qiu A C 2008 *Proc.17th Int. Conf. High Power Particle Beams* (Xi'an: Conf. High Power Particle Beams) p. 14

[10] Wu G, Qiu A C, Lü M, Hei D W, Sheng L, Wei F L, Kuai B, Wang L P, Cong P T, Lei T S, Han J J and Sun T P 2009 *High Power Laser Particle Beams* **21** 1115

[11] Hall G N, Pikuz S A, Shelkovenko T A, Bland S N, Lebedev S V, Ampleford D J, Palmer J B A, Bott S C, Rapley J and Chittenden J P 2006 *Phys. Plasmas* **13** 082701

[12] Gan X S, Yang J M, Yi R Q, Zhang J Y, Zhao Y D, Zhao Y, Cui M Q and Deng A H 2007 *High Power Laser and Particle Beams* **19** 1827

[13] Yang J M, Gan X S, Zhao Y, Cui M Q, Zhu T, Zhao Y D, Sun L J, Zheng L, Yan F, Hu Z M, Wei M X, Zhang J Y and Yi R Q 2011 *Chin. Phys.* B **20** 010705

[14] Henke B L, Gullikson E M and Davis J C 1993 *At. Data Nucl. Data Tables* **54** 181

[15] Marshall F J, Knauer J P, Anderson D and Schmitt B L 2006 *Rev. Sci. Instrum.* **77** 10F308

[16] Knauer J P, Marshall F J, Yaakobi B, Anderson D, Schmitt B A, Chandler K M, Pikuz S A, Shelkovenko T A, Mitchell M D and Hammer D A 2006 *Rev. Sci. Instrum.* **77** 10F331

[17] Scholze F, Rabus H and Ulm G 1996 *Proceedings of the SPIE* (Denver: Proc. SPIE) **2808** 534

[18] Idzorek G C and Bartlett R J 1997 *Proceedings of the SPIE* (San Diego: Proc. SPIE) **3114** 349

[19] Apruzese J P, Whitney K G, Davis J and Kepple P C 1997 *J. Quantum Spectrosc. Radiat. Transfer* **57** 41